Twelve-Membered *O*-Bridged Cyclic Ethers of Red Seaweeds in the Genus *Laurencia* Exist in Solution as Slowly Interconverting Conformers

Graziano Guella,* Giuseppe Chiasera, Ines Mancini, Aysel Öztunç and Francesco Pietra*

Abstract: The twelve-membered *O*-bridged cyclic ether obtusallene IV (**1**), a new isolate from the red seaweed *Laurencia obtusa* from Kaş in the Turkish Mediterranean, revealed temperature-dependent NMR signals attributable to a major conformer in equilibrium with a minor conformer by 180° flipping of the *trans* olefinic bond. This prompted us to reexamine the known congeners obtusallene I (**2**), 10-bromoobtusallene I (**3**), obtusallene II (**4**), and obtusallene III (**5**), isolated both from the same and taxonomically related seaweeds, as well as their semisynthetic derivative peracetylobtusallene III (**6**). Two conformers could in fact be directly observed at room temperature for **2**–**3** and at low temperature for **4**. Marked cross-saturation-transfer effects between the couples of conformers confirmed these observations. Activation energies for processes involving 10-membered subunit rings (**2**–**3**) are higher than for 11-membered (**4**–**5**) analogues, where faster conformational motion occurs too resulting in mediated vicinal *J* couplings. 1,3-Dihydroxy substituents in **5** form an intramolecular hydrogen bond in low-polarity, non-H-bonding solvents; this results in the existence of two further conformers, giving more complex NMR spectra. Descriptions in the literature of single conformers for obtusallenes **2**–**5** must have resulted from overlooking minor NMR signals or attributing them to impurities.

Keywords
conformation analysis · heterocycles · hydrogen bonds · NMR spectroscopy · obtusallenes

Introduction

Polyether acetogenins isolated from marine dinoflagellates have recently attracted much attention for their ecotoxicity[1] and other potent biological activities,[2] as well as for their unusual array of *O*-heterocycles of various sizes. Red seaweeds in the genus *Laurencia* are the only other organisms that rival the dinoflagellates in imagination as builders of unusual cyclic ethers, some of which are transferred through the diet to herbivorous opisthobranch molluscs[3] and show potent biological activity, including cytotoxicity towards tumour cells. The interest in all these cyclic ethers, together with Paclitaxel®-type compounds,[4] has revived methods for the synthesis of medium rings.[5]

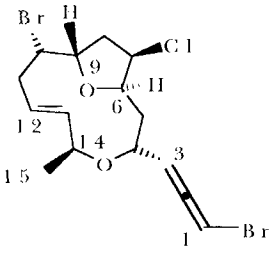

1

The C_{15} acetogenins from *Laurencia* spp. include such oddities as branched oxepanes[6] and *O*-bridged twelve-membered cyclic ethers.[7] A central example in the latter series is obtusallene I (**2**), isolated from *Laurencia obtusa* collected at Gökceada in the Aegean Sea[7a–e] and described as having in solution[7d] the single conformation seen in the crystal (**2**, i.e., C6 up and C5 down).[7b] Other members of this family, 10-bromoobtusallene I (**3**),[7d] obtusallene II (**4**)[7c] and obtusallene III (trivial name coined here) (**5**)[7c] were similarly described.

We recently isolated a new obtusallene from a sample of *L. obtusa* collected near Kaş to which the name obtusallene IV (**1**) was assigned. The NMR spectrum of **1** showed resonances attributable to equilibrating conformers, in sharp contrast to previous single-conformer descriptions for compounds of this class in solution.[7d] Because of the importance of conformational phenomena in recognition interactions with receptors, we decided to reexamine previous cases.[7]

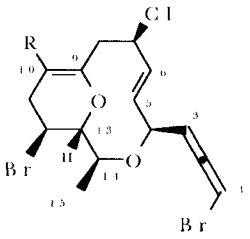

2 R = H
3 R = Br

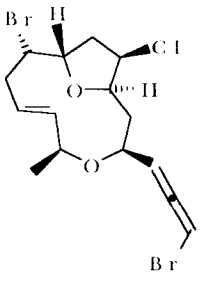

4

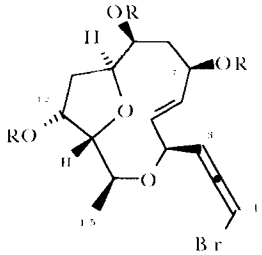

5 R = H
6 R = Ac

[*] Prof. F. Pietra, Dr. G. Guella, Dr. G. Chiasera, Dr. I. Mancini
Laboratorio di Chimica Bioorganica, Facoltà di Scienze MFN
Università di Trento, I-38050 Povo-Trento (Italy)
Fax: Int. code +(461)882-009
e-mail: fpietra@discat.unipi.it
Dr. A. Öztunç
Faculty of Pharmacy, University of Istanbul, Istanbul (Turkey)

  0947-6539/97/0308-1223 $ 17.50+.50/0

Table 1. ^{1}H NMR spectra (21 °C) for obtusallene IV (**1**) in C_6D_6 and for obtusallene I (**2**) and 10-bromoobtusallene I (**3**) in $CDCl_3$

H atom	Obtusallene IV (**1**) **1**	Obtusallene I (**2**): **2a**/**2b** = 4:1 **2a**	**2b**	10-Bromoobtusallene I (**3**): **3a**/**3b** = 3:1 **3a**	**3b**
1	5.63 dd (J(1,3) = 5.6, J(1,4) = 1.7)	6.07 (dd,1.8,5.7)	6.09 (br d, 6.0)	6.08 (dd, 1.9,5.9)	6.09 (dd, 2.0,5.8)
3	5.07 dd (J(3,1) = 5.6, J(3,4) = 6.7)	5.56 (t, 5.7)	5.52 (m)	5.54 (t, 5.9)	5.51 (t, 5.8)
4	4.06 tdd (J(4,1) = J(4,5α) = 1.7, J(4,3) = 6.7, J(4,5α) = 10.8)	4.47 (dt, 1.8,5.7)	[a]	4.47 (dt, 2.0,5.9)	[a]
5	α) 1.40 ddd (J(5α,6) = 2.0, J(5α,4) = 10.8, J_{gem} = 13.6)	5.94 (dd,5.7,15.9)	5.83 (dd, 6.0,15.9)	5.98 (dd, 5.9,15.7)	5.91 (dd, 7.3,15.9)
	β) 1.70 ddd (J(5α,4) = 1.7, J(5β,6) = 10.5, J_{gem} = 13.5)				
6	3.49 ddd (J(6,5α) = J(6,7) = 2.0, J(6,5β) = 10.5	6.21 (dd,10.5,15.9)	[a]	6.20 (dd, 10.6,15.7)	[a]
7	3.67 dd (J(7,6) = 2.0, J(7,8α) = 4.9	4.23 (dt,6.3,10.5)	4.37 (td, 6.9,10.6)	4.43 (dt, 5.9,10.6)	4.83 (td, 7.1,10.3)
8	α) 1.78 m	2.81 (dd, 6.3,13.3)	2.97 (dd, 6.9,13.3)	3.36 (dd, 5.9,13.2)	3.35 (dd, 7.1,13.3)
	β) 2.13 dd (J(8β,9) = 7.1, J_{gem} = 14.4)	2.46 (dd, 10.5,13.3)	[a]	2.44 (dd, 10.6,13.3)	2.61 (dd, 10.3,13.6)
9	4.57 ddd (J(9,8β) = 7.2, J(9,8α) = 9.4, J(9,10) = 5.3)	–	–		–
10	3.95 dd (J(10,9) = 5.3, J(10,11β) = 3.8, J(10,11α) = 11.7)	4.60 (td, 1.5,5.1)	4.61 (m)	–	–
11	α) 1.98 ddd (J(11α,10) = 11.7, J(11α,12) = 10.5, J_{gem} = 14.4	2.47 (ddd, 1.5,5.1,19.1)	[a]	2.89 (dd, 5.2,18.7)	[a]
	β) 2.42 ddd (J(11β,10) = 3.8, J(11α,12) = 1.7, J_{gem} = 14.4)	2.33 (qdd, 1.5,5.1,19.1)		2.67 (qd, 1.6,18.7)	[a]
12	5.19 m	4.22 (ddd, 1.5,1.7,5.1)	[a]	4.20 (td, 1.6,5.4)	[a]
13	5.19 m	3.97 (dd, 1.8,9.3)	[a]	3.99 (td, 1.8,9.3)	[a]
14	4.17 m	3.62 (qd, 6.3,9.3)	3.49 (qd, 6.4,8.7)	3.61 (qd, 6.5,9.3)	3.47 (qd, 6.5,8.7)
15	1.13 d (J(15,14) = 7.0)	1.10 (d, 6.3)	1.11 (d, 6.4)	1.16 (d, 6.5)	1.13 (d, 6.5)

[a] Signal overlapped by the resonance of the major conformer. NOE effects from NOE2D experiments for obtusallene IV (**1**): H4 with H3, H_β5 and H_γ15; H_γ5 with H6 and H7; H6 with H_α8, H12 or H13; H9 with H_β8 and H10; H10 with H9, H_β11 and H12 or H13; H_γ15 with H4, H14 and H12 or H13 (see also Experimental Procedure).

Results and Discussion

Obtusallene IV (1): HRMS-EI for **1** was carried out on the intense heavy-halogen-bearing fragment ion deriving from loss of the bromoallene functionality, which is supported by the characteristic ^{13}C NMR resonances δ_C = 73.70 d, 200.74 s and 103.32 d. This information, together with that on a fragment ion attributable to Br loss from the molecular ion, and atom counts from NMR spectra, led to the composition $C_{15}H_{19}Br_2ClO_2$ for the whole molecule, implying five unsaturated bonds. Two cycles were suggested by evidence of an *E* olefinic bond, positioned as shown in **1** on the basis of COSY experiments and differential decoupling. This and H4/C3 and H14/C15 correlations from HMBC experiments also support the allene–C4–O–C14–Me fragment (Table 1), establishing a 12-membered *O*-heterocycle of the obtusallene[7] type. Characteristic δ_C values for C6 and C9 (Table 2), assigned by HMQC and long-range H6/C9 coupling provide support for the existence of the tetrahydrofuran moiety. On similar evidence both chlorine (δ_{C7} = 62.48 d) and bromine (δ_{C10} = 49.88 d) were assigned positions. Thus, obtusallene IV (**1**) must be a stereoisomer of obtusallene II (**4**).[7c] Starting from arbitrarily β-positioned C15, the α position for C3 rests on strong positive H_γ15/H4 NOE. Support for H_α6 is given by the large coupling constant $J_{5\beta,6}$ = 10.5 Hz, while H_β5 is defined by the strong NOE with H4. H6/H7 and H9/H10 NOEs support these cisoid relationships, as well as transoid H6/H9. This, and an upfield δ_{C4} for **1** (Table 2) with respect to the same carbon atom in **4**, resulting from the γ-gauche effect of C15 on C4, establish **1** as the C4 epimer of **4**; this γ-gauche effect is also well known for the oxepanes extracted from these seaweeds.[6]

Table 2. ^{13}C NMR spectra (21 °C) for obtusallene IV (**1**) in C_6D_6 and for obtusallene I (**2**) and 10-bromoobtusallene I (**3**) in $CDCl_3$.

Atom	Obtusallene IV **1**	Obtusallene I (**2**): **2a**/**2b** = 4:1 **2a**	**2b**	10-Bromoobtusallene I (**3**): **3a**/**3b** = 3:1 **3a**	**3b**
C(1)	73.5 d	74.16 d	74.16 d	74.34 d	74.28 d
C(2)	201.08 s	202.16 s	202.26 s	202.20 s	202.28 s
C(3)	104.27 d	100.09 d	99.81 d	99.78 d	99.62 d
C(4)	65.05 d	69.88 d	69.70 d	69.73 d	69.73 d
C(5)	38.77 t	129.03 d	130.60 d	129.42 d	130.67 d
C(6)	76.64 d	139.74 d	136.42 d	140.24 d	136.76 d
C(7)	62.70 d	59.49 d	52.72 d	56.49 d	49.52 d
C(8)	37.58 t	43.33 t	42.60 t	42.53 t	43.12 t
C(9)	78.24 d	147.77 s	148.27 s	145.82 s	145.16 s
C(10)	0.48 d	95.20 d	95.79 d	94.13 s	94.96 s
C(11)	37.82 br t	26.99 t	26.90 t	36.65 t	36.56 t
C(12)	[a]	41.61 d	41.92 d	41.92 d	42.07 d
C(13)	[a]	81.83 d	82.29 d	81.89 d	82.46 d
C(14)	70.19 d	68.40 d	68.40 d	68.20 d	68.20 d
C(15)	14.11 q	16.43 q	17.16 q	16.56 q	17.22 q

[a] Overlapped by the solvent residual signals.

Given the absolute configurations assigned to obtusallene I (**2**)[7b] and obtusallene II (**4**)[7c] from X-ray diffraction data, the existence of a positive Cotton effect for **1** and negative ones for all other obtusallenes lets us assign the *S* configuration to the bromoallene sidechain in **1** and the *R* configuration in all other cases.

As anticipated, broad NMR signals were observed for **1** at room temperature in $CDCl_3$, in particular ^{13}C signals for C11–C15 (15–20 Hz linewidth) as well as C4, C9 and C10 (8–12 Hz). When the temperature was lowered to 0 °C signal sharpening occurred, and the slow exchange limit was reached at about −20 °C, where only the dominant conformer was observed. On raising the temperature, we observed sharpening at +50 °C for only some signals, while other signals, in particular for C11–C15, were still far from the fast exchange limit. Similar conclusions were drawn from variable-temperature ^{1}H NMR spectra for **1**, which also showed invariance of the proton coupling pattern regardless of temperature, in the range from −40 to +50 °C, or the solvent, $CDCl_3$ or C_6D_6.

These phenomena suggest that these processes involve slow equilibria between at least two conformers, the minor one(s) so scarcely populated (and therefore having quite broad weak signals) as to escape direct detection. The minor conformer(s) must be sufficiently populated, however, to affect the resonances for the major conformer, particularly those for the C12=C13 olefinic bond and the C10–C13 and C12–C14 portions, as suggested from the change of sign of the average value for dihe-

0947-6539/97/0308-1224 $ 17.50+.50/0 Chem. Eur. J. 1997, 3, No. 8

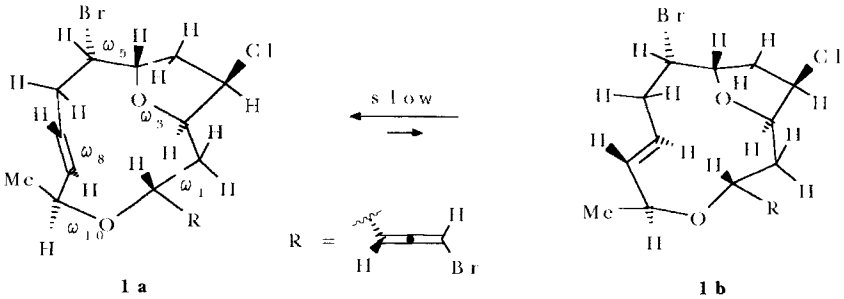

Scheme 1. Major (**1a**) and minor (**1b**) conformers of **1**.

dral angles C10-C11-C12-C13 (ω_7, see Scheme 1) and C12-C13-C14-O (ω_9) during C12=C13 flipping (D process[8]). Cross-saturation-transfer experiments[9] could not be carried out at 300 MHz in this case as crowding of signals leaves no signal-free zone in which to probe the system.

In a more polar solvent, CD_3OD, at room temperature all ^{13}C signals proved to be sharper (6–11 Hz) than the corresponding signals in either $CDCl_3$ or C_6D_6 (15–20 Hz), ruling out any effect of selective broadening at the exchange sites in the more polar solvent. Clearly in the more polar solvent the contribution of the minor conformer has decreased further.

Molecular mechanics (MM) calculations supported the existence of only two conformers, major **1a** and minor **1b**, within an energy window of 3 kcal mol^{-1} (Scheme 1). Conformer **1a** rests on a +9% NOE observed on either H13 or H_γ15 in the low exchange limit (−20 °C) on irradiation at H6 or H12, respectively. The MM-calculated relative weight of **1b**, 35%, was not in agreement with NMR observations, which rather pointed to a negligible contribution of this conformer. This discrepancy must be attributed to lack of suitable MM parameters for compounds in this class. In fact, unparametrized MM calculations led to the dramatically wrong conclusion that **1b** is the major conformer, while parametrization[10] improved the simulation somewhat as indicated above. Any further lengthy refinement of parameters to get MM calculations fitting with the experiments is immaterial for the present conclusions and thus was not attempted.

The coupling data in Table 3, calculated from extended Karplus relationships,[11] also suggest that **1b** is the minor conformer. Fair agreement between calculated and observed ^3J couplings for **1a** (Table 3) shows that this conformer is the one predominantly populated in nonpolar solvents and becomes practically the sole conformer on changing to polar solvents. The geometric parameters are summarized in Table 4; the other obtusallenes are included.

These observations prompted us to examine the other obtusallenes reported in the literature,[7] for which no dynamic NMR phenomena had been described. We hoped to arrive at a general picture of the conformational behaviour of these bridged twelve-membered rings.

Obtusallene I (2) and 10-bromoobtusallene I (3): The ^1H NMR spectrum of obtusallene I (**2**) in $CDCl_3$ at +21 °C (Table 1) showed a series of minor peaks that, from saturation-transfer experiments,[9] could be attributed to the minor conformer **2b** in slow exchange with the major conformer **2a** (Scheme 2). Saturation transfer was as large as 30–35% on irradiating either H_α8 or 14H of **2b** while observing the corresponding signals of **2a**. An 85:15 **2a**/**2b** population ratio was established by ^1H NMR integration of signals under complete relaxation. ^{13}C NMR spectra (Table 2) led to the same conclusions. Conformation **2a** matches the one already described by both X-ray diffraction techniques in the crystal[7a,b] and NMR experiments in solution,[7a,d] while **2b** had escaped previous attention.[7a,d] 10-Bromoobtusallene II (**3**),[7d] isolated from a sample of *L. obtusa* collected at Kaş, showed similar behaviour with a 72:28 **3a**/**3b** population ratio (Tables 4 and 5). Like **2b**, **3b** had escaped previous attention.[7d]

This conformational behaviour could be nicely simulated by MM calculations: **a**-type conformers were calculated to be more stable than **b**-type conformers by 1.25 or 1.05 kcal mol^{-1} for

Table 3. Experimental and calculated ^3J couplings for obtusallene IV (**1**) and obtusallene I (**2**).

Relevant vicinal protons	Calcd ^3J (Hz) [a] **1a**	**1b**	Experimental ^3J (Hz) (21°), C_6D_6 **1a** ⇌ **1b**	Calcd ^3J (Hz) [a,b] x_a/x_b% = 87/13 [c] **2a**	**2b**	Experimental ^3J (Hz) (21°), $CDCl_3$ x_a/x_b% = 87/13 [c] **2a**	**2b**
H4–H_α5	11	11.5	10.8	6.6	11.4	5.7	[f]
H4–H_β5	1.4	1.9	1.7	–	–	–	–
H_α5–H6	1.7	2.1	2	–	–	–	–
H_β5–H6	11.4	11.6	10.8	–	–	–	
H6–H7	2.1	2.1	2	11.6	6.6	10.5	6.9
H7–H_α8	5.1	5.4	4.9	5.5	6.7	6.3	6.9
H7–H_β8	1.6	1.5	1	10.9	10.1	10.5	10.6
H_α8–H9	10.2	10.1	9.4	–			
H_β8–H9	6.5	6.7	7.2		–		–
H9–H10	5	3.8	5.3	–	–	–	–
H10–H_α11	11.8	11.5	11.7	2.9	2.9	1.5	[f]
H10–H_β11	3.8	4.4	3.8	4.9	4.8	5.1	[f]
H_α11–H12	11.6	6.3	10.5	4.2	4.1	5.1	[f]
H_β11–H12	3.2	2.7	1.6	2.3	2.3	1.5	[f]
H12–H13	–	–	–	1.5	1.6	1.7	[f]
H13–H14	4.8	8.5	5.1 [e]	9.0	8.4	9.3	8.7

[a] Evaluated by *PCMODEL* 4.0 subroutine based on modified Karplus equation[11] observed coupling patterns from ^1H NMR in $CDCl_3$ at 21 °C. [b] The same analysis was performed on 10-bromoobtusallene I (**3**) and gave similar results. [c] Molar ratio of **a** and **b** conformers calculated from the equation $x_a = [1+\exp(-\Delta E/RT)]^{-1}$ where ΔE is the difference in strain energies between **b** and **a** conformers at $T = 298$ K. [d] Molar ratio of **a** and **b** conformers determined by NMR signal integration. [e] In $CDCl_3$ at RT. [f] ^3J could not be assigned because of signal overlapping (Table 4).

Table 4. Endocyclic torsional angles for compounds **1**–**5** in the most populated conformations.

Calcd conf. [a]	Rel. strain energy	Endocyclic torsional angles as obtained by MM calculations [b]										
		ω_1	ω_2	ω_3	ω_4	ω_5	ω_6	ω_7	ω_8	ω_9	ω_{10}	ω_{11}
1a	0.0	+71	+60	+166	+122	−54	+60	**−122**	**+173**	**−107**	+77	−120
1b	+0.5	+63	+56	+167	+119	−67	+54	**+39**	**−174**	**+75**	+66	−127
2a	0.0	**+60**	**−167**	**+107**	−46	+81	−167	+86	+57	−129	+61	–
2b	+1.2	**−106**	**+169**	**−53**	−36	+96	−163	+84	+67	−114	+65	–
4a	0.0	−67	+89	+165	+119	**−50**	**+62**	**−127**	**+170**	**−71**	−75	+124
4b	+1.5	−74	+81	+168	+116	**−58**	**+55**	**+37**	**−171**	**+100**	−86	+120
4c	+2.7	−81	+55	+165	+120	**+57**	**−40**	**−76**	**+171**	**−63**	−79	+140
4d	+0.5	−136	+59	+100	+176	**+75**	**−48**	**+98**	**−178**	**+123**	−67	+102
4e	+1.3	−94	+48	+161	+126	**+54**	**−59**	**+98**	**−170**	**+109**	−86	+131
5a	+1.0	**−103**	**+175**	**−53**	**−70**	**+54**	+52	+170	+106	+54	−111	+77
5b	+1.5	**+61**	**−174**	**+130**	**−79**	**+43**	+52	+168	+102	+48	−124	+66
5c	0.0	**−132**	**+175**	**−103**	**+61**	**−89**	+63	+107	+167	+81	−73	+81
5d	+1.0	**+36**	**−178**	**+75**	**+53**	**−99**	+52	+103	+169	+77	−87	+78

[a] See Schemes 1–4. [b] Where the conformers differ markedly in dihedral angle values the entry is emphasized in boldface.

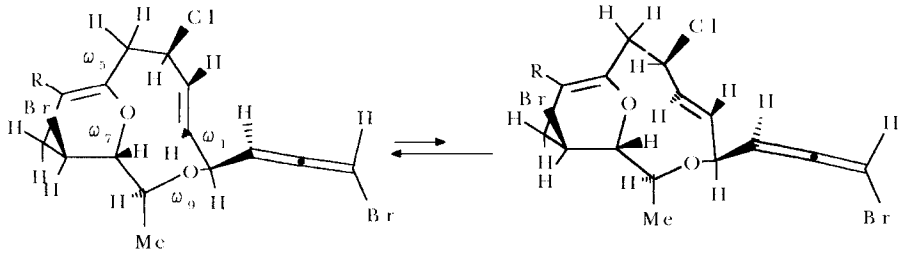

Scheme 2. Major (**2a**, **3a**) and minor (**2b**, **3b**) conformers of **2** and **3**.

either **2** or **3**, corresponding to 90:10 or 85:15 population ratios, respectively (Table 3). Such a behaviour may be explained by conformational changes involving 180° flipping (D process) of the *trans* olefinic bond; in support, the largest $\Delta\delta_C$ is at C7 for each couple of conformers (Table 2). The data in Table 3 show excellent agreement between calculated[11] and experimental vicinal J couplings for conformers **2a** and **2b**. Notably, the value of $J_{6,7}$ is characteristic of each conformer (Table 3) and can therefore be taken as a conformational probe. That the stability of **2b** is lower than that of **2a** may be attributed to torsional strain arising from eclipsing in the C6–C9 zone, with a C6-C7-C8-C9 (ω_4) torsional angle of −36°.

Obtusallene II (4): Obtusallene II (**4**), isolated not only from *L. obtusa* from the Aegean and Mediterranean coasts of Turkey[7c] but also from *L. microcladia* of Il Rogiolo on the coast of Tuscany (Experimental Procedure), showed temperature-dependent NMR spectra that could not be rationalized by a D process only. Broad resonances for **4**, like those of **1**, instead of the two series of sharp resonances for both **2** and **3**, were

Table 5. Calculated and experimental ^3J values for obtusallene II (**4**) and obtusallene III (**5**).

Conformer	x_i [a]	Vicinal J coupling [b]													
		4,5α	4,5β	5α,6	5β,6	6,7	7,8α	7,8β	8α,9	8β,9	9,10	10,11α	10,11β	11α,12	11β,12	13,14
4a	0.33	1.8	11.5	1.1	8.7	2.0	5.1	1.6	10.1	6.6	5.4	11.9	3.7	11.4	3.0	6.3
4b	0.10	1.4	11.2	1.0	9.9	2.0	5.4	1.5	9.8	7.0	4.6	11.6	4.3	6.2	2.7	10.8
4c	0.02	1.0	10.0	2.2	11.6	2.2	5.6	1.4	9.7	6.9	1.2	1.8	5.2	7.4	6.0	6.5
4d	0.40	8.6	1.3	1.5	11.3	7.1	6.5	1.2	11.7	3.1	0.7	2.4	4.5	4.4	10.7	11.6
4e	0.15	1.1	8.9	3.0	11.6	2.3	5.4	1.5	10.4	6.3	1.4	3.7	2.8	4.4	10.9	11.5
4 [c]	–	4.4	6.9	1.4	10.3	4.2	5.8	1.4	10.6	5.2	2.4	5.5	4.4	7.4	6.9	8.6
4 [d,e]	–	3.8	7.5	1.9	9.5	4.3	6.0	~0	8.6	6.0	4.2	6.9	4.4	6.9	6.7	8.2
		4,5	6.7	7,8α	7,8β	8α,9	8β,9	9,10	10,11α	10,11β	11α,12	11β,12	12,13	13,14		
5a	0.40	11.4	6.6	2.9	10.6	5.1	11.6	1.0	3.3	11.7	1.3	5.1	5.9	9.5		
5b	0.05	6.6	11.4	2.0	9.4	6.6	11.5	1.0	3.4	11.7	1.2	5.8	6.4	9.6		
5c	0.40	11.2	4.6	2.6	4.0	0.9	7.9	0.5	8.2	8.5	1.4	5.3	1.6	7.5		
5d	0.15	7.3	7.3	3.4	3.2	1.3	9.1	1.0	8.8	7.5	1.2	6.0	1.7	7.9		
5 [c]	–	10.4	6.1	2.8	6.8	2.9	9.7	0.9	6.1	9.8	1.3	5.3	3.6	8.5		
5 [d,e]	–	8.6	3.7	2.5	8.1	2.5	8.1	≈0	5.9	9.0	1.6	5.0	3.8	8.1		
5 [e,f]	–	[g]	5.0	2.1	10.4	4.7	10.4	≈0	4.0	10.5	≈0	5.5	5.8	8.0		

[a] x is the estimated molar ratio (see text). [b] Evaluated by PCMODEL 4.0 subroutine based on modified Karplus equation.[11] [c] Evaluated in the fast exchange limit from $J(m,n) = \Sigma_i x_i J_i(m,n)$. [d] Experimental J patterns from ^{1}H NMR in $CDCl_3$ at 50° (fast exchange limit). [e] Experimental values; all others are calculated. [f] As [d], except for CD_3OD as solvent. [g] Overlapped signal.

0947-6539/97/0308-1226 $ 17.50+.50/0 Chem. Eur. J. 1997, 3, No. 8

observed at +19 °C, and further line broadening was observed on lowering the temperature to 0 °C; when the temperature was raised to +40 °C line sharpening resulted. It was only on lowering the temperature to −70 °C that doubling of many NMR signals of **4** could be observed, indicative of a slow exchange between two conformers in a population ratio of ca. 1:2. In agreement with this observation, a nearly 100% cross-saturation-transfer[9] was observed at −40 °C for many resonances of **4**, in particular on irradiation of $\delta_H = 4.77$ td for the minor conformer while observing the resonance at $\delta_H = 3.95$ m for the major conformer (H9). COSY maps, obtained at −60 °C, enabled us to assign the resonances for each conformer. The ^{1}H-decoupled ^{13}C spectrum at −50 °C also showed signals for two conformers; their resonances were tentatively assigned on the basis of room-temperature HMQC experiments only (Experimental Procedure) since this is immaterial for the present work.

It should also be noted that at a lower temperature, −64 °C, the ^{13}C NMR signals for the major conformer (**4d**) are significantly broader than for the minor conformer (**4a**), in some cases by as much as 3–5 times.

A report about sharp ^{1}H NMR signals at 360 MHz for **4** at unstated temperature,[7e] thus assumed by us to be room temperature, contrasted with our observations at lower field, 300 MHz. Our suspicion that the higher-field experiments had been performed at a higher temperature was justified: laboratory notes were traced by one of the previous authors, A.Ö., indicating +55 °C as the temperature for the 360 MHz experiments on **4**.

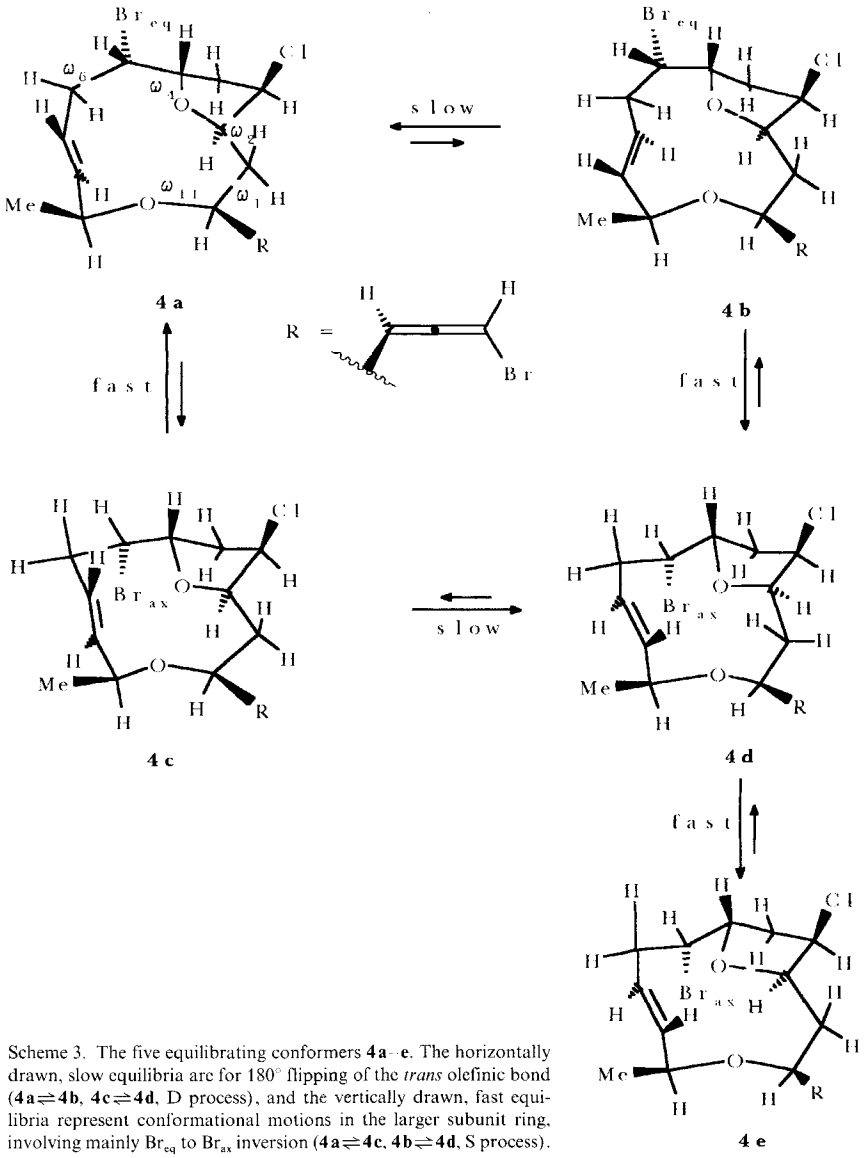

Scheme 3. The five equilibrating conformers **4a**–**e**. The horizontally drawn, slow equilibria are for 180° flipping of the *trans* olefinic bond (**4a**⇌**4b**, **4c**⇌**4d**, D process), and the vertically drawn, fast equilibria represent conformational motions in the larger subunit ring, involving mainly Br_{eq} to Br_{ax} inversion (**4a**⇌**4c**, **4b**⇌**4d**, S process).

On careful analysis of the coupling pattern for selected protons of **4**, either under slow exchange (−45 °C) or fast exchange (+55 °C) conditions, further divergence from the behaviour of **2** and **3** emerged, requiring an interplay among four equilibrating conformers **4a**–**d**. This is shown in Scheme 3, where the horizontally drawn, slow equilibria are for 180° flipping of the *trans* olefinic bond, which brings about the exchange either between major **4a** and minor **4b**, or between minor **4c** and major **4d** (D processes).[8] The vertically drawn, fast equilibria represent conformational motions in the larger subunit ring, involving mainly Br_{eq} to Br_{ax} inversion on going from major **4a** to minor **4c** or from minor **4b** to major **4d** (S processes).[8] This explains the values $J(4,5\alpha) = 3.8$, $J(4,5\beta) = 7.5$, $J(10,11\alpha) = 6.9$, and $J(11\beta,12) = 6.7$ Hz, while on account of **4a** and **4b** alone corresponding values of ca. 1.5, 11.0, 11.0, and 3.0 Hz would have been expected (Table 5). Since S-process equilibria remained fast at −45 °C, the above observed 1:2 ratio of conformer populations implies that the sum of populations **4a**+**4c** must be half of **4b**+**4d**. Being in the conditions of the low exchange limit for D processes and the fast exchange limit for S processes, H7 and H9 may be taken as optimal conformational probes through which to evaluate the relative weights of **4a**/**4c** and **4b**/**4d**, respectively. ^{1}H NMR patterns were well-defined for H9 [at $\delta_H = 4.77$, with coupling pattern td $J(9,8\beta) \approx J(9,10) = 6.3$, and $J(9,8\alpha) = 8.5$ in fair agreement with that for **4a**, Table 5 and Experimental Procedure] in the **4a**/**4c** couple. They were also well defined for H7 [at $\delta_H = 4.62$, with coupling pattern brt, $J(7,6) \approx J(7,8\alpha) = 6.2$, and $J(7,8\beta) \approx 0$, in fair agreement with that for **4d**, Table 5 and Experimental Procedure] in the **4b**/**4d** couple. These two observations indicated that **4a** and **4d** are the more populated conformers.

MM calculations were carried out with an appropriate force field for compounds of this type, MMX, and the conformational space was searched. Five conformers emerged, **4a**–**4d** described above and **4e**, which differs from **4d** mainly in the values of the dihedral angles $\omega 3$ and $\omega 4$ (Table 3), corresponding to a S-type flipping of the tetrahydrofuran oxygen atom. The latter is indicated to be cisoid to O–C4 in all conformers except **4d**, where it is transoid. MM calculations were also carried out on a simplified model having a methyl group in place of the allene side chain. In fact, any overcomplication arising from the conformational properties of the latter proved irrelevant to the

conformational properties of the ring; the number of significant conformers and their geometry and relative stability were not affected by the replacement of the allene side chain by a methyl group. Thus, for R = methyl but extrapolating to R = bromoallene, the calculated relative weights of the conformers turned out to be in the order **4a** 60% > **4d** 27% > **4e** 7% ≈ **4b** 5% > **4c** 1%. By this treatment the MM calculations correctly emulated the experimental observation that **4a** is more populated than **4c**, while **4d** is more populated than **4b** and **4e**. However, the MM calculations failed to reproduce correctly the condition **4a**+**4c** = $^1/_2$(**4b**+**4d**+**4e**) observed in the slow exchange limit of the D processes. Very likely this reflects incomplete parametrization of the MM program. Anyway, from Table 5, last row, the population distribution that best matches the experimental results (**4a**:**4b**:**4c**:**4d**:**4e** = 0.33:0.10:0.02:0.40:0.15) allowed us to calculate *J* values through extended Karplus relationships[11] for all protons of **4** in generally good agreement with those observed under conditions of fast exchange in either $CDCl_3$ (Table 5) or the more polar CD_3OD. The discrepancy between calculated and experimental values proved larger than 1 Hz only for the H8–H10 *J* values, probably due to fast flipping of envelope forms of the tetrahydrofuran ring. This agrees with the NMR experiments described above: at such low temperatures, where S processes are also slowed down, the ^{13}C resonances for the major form (**4b**+**4d**+**4e**) are expected to undergo a larger broadening than for the minor form (**4a**+**4c**). In the former case, in fact, three conformers begin to take equal weight, while in the latter case practically only **4a** is populated by the S process, thereby being dynamically insensitive to further lowering of the temperature.

Obtusallene III (5) and **peracetylobtusallene III (6)**: For practical reasons we have assigned a trivial name to both **5** (obtusallene III), isolated from the above Kaş sample of *L. obtusa*, and semisynthetic **6** (peracetylobtusallene III)[7c] which had no common names. Consequently **1** was called obtusallene IV. The conformational behaviour of **5** in $CDCl_3$ was monitored by dynamic ^1H NMR at probe temperature +50 °C; sharp signals were observed, as previously reported for spectra taken at higher field and lower temperature (360 MHz and room temperature).[7c] In contrast, ^{13}C NMR spectra consisted of quite broad signals, some actually under coalescence conditions. As in the case of **4**, these NMR spectral features could be accounted for by 180° flipping of the *trans* olefinic bond, by which the major conformer **5a** (which corresponds to the form in the crystalline state[7c]) undergoes slow exchange with the minor conformer **5b**. Averaging of vicinal *J* couplings suggests that in the couples of conformers **5a**/**5c** and **5b**/**5d** rapid exchange occurs. In Scheme 4 this is represented by the vertically drawn equilibria, which involve a change from equatorial to axial hydroxyl groups (S process), while slow exchange within the couples of conformers **5a**/**5b** and **5c**/**5d** is represented in the horizontally drawn equilibria (S process) in Scheme 4. The position of the tetrahydrofuran oxygen atom, up in **5a** and **5b** and down in **5c** and **5d** (Scheme 4), as indicated by MM calculations, determines quite different torsion angles H10-C10-C11-H_α11 and H10-C10-C11-H_β11 in the four conformers as well as an averaged coupling pattern for H-10 (Table 5). Were it not for a slightly faster time scale, this conformational behaviour would resemble the one described for **4** in Scheme 3. On closer inspection, however, several peculiarities emerged for **5**. First, its NMR spectra failed to reveal any splitting of the signals even at low temperature, implying that the minor conformers are not populated enough to be directly observable by NMR, but are sufficiently populated to affect the line shape of the observable conformers.

A more striking oddity emerged on replacing $CDCl_3$ with CD_3OD as solvent; in the latter the conformational behaviour of **5** could be accounted for in terms of two conformers only, major **5a** and minor **5b**. This experiment was suggested by the results of MM calculations, which indicated **5c** as the most populated conformer when the dielectric constant for $CDCl_3$ was used, while when the dielectric constant for CD_3OD was used an equilibrium between **5a** and **5b** was suggested, in accordance with the experimental observations. The whole body of these observations may be rationalized by acknowledging that a low-polarity solvent like $CHCl_3$ favours intramolecular H-bonding in the 1,3-diol moiety, bringing two new conformers (**5c** and **5d**) into play. A polar, H-bonding solvent like MeOH is capable of disrupting the intramolecular hydrogen bonds, leaving only **5a** and **5b** in play, which results in simpler NMR spectra. With **5** in $CDCl_3$ under conditions of fast exchange (+50 °C), the ^1H NMR coupling pattern for either H_β8 or H10 (Table 5) could not be accounted for by conformations **5a** and

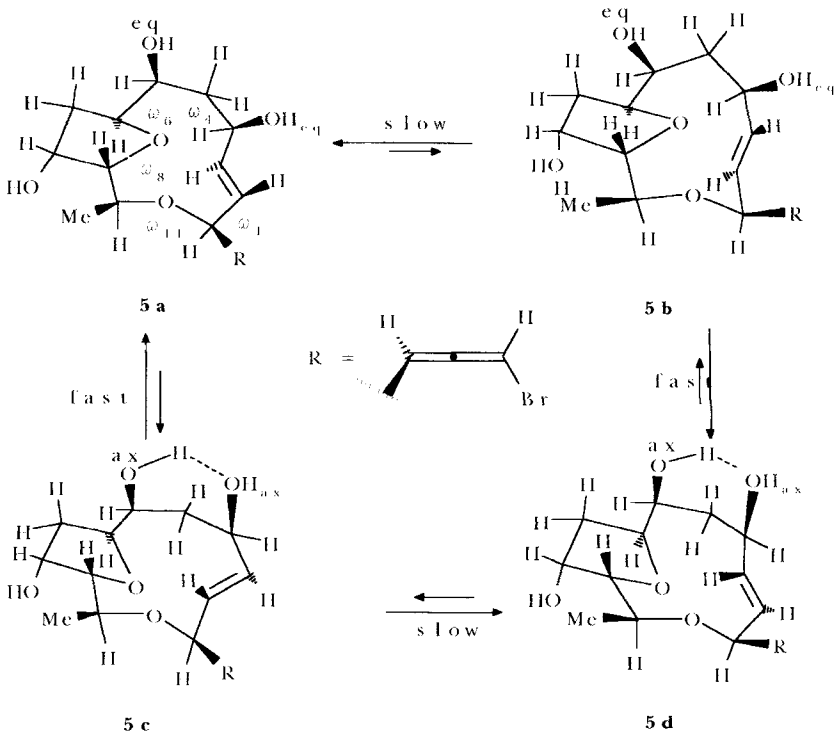

Scheme 4. Conformers **5a**/**5c** and **5b**/**5d** undergo rapid exchange (vertically drawn equilibria), which involves a change from equatorial to axial hydroxyl groups (S process), while exchange within the couples of conformers **5a**/**5b** and **5c**/**5d** is slow (horizontally drawn equilibria, S process).

0947-6539/97/0308-1228 $ 17.50+.50/0 Chem. Eur. J. 1997, 3, No. 8

5b alone. Relative abundances in Table 5 were obtained as the set of values that, under conditions of fast exchange, gave calculated[11] vicinal J values in best agreement with the experimental data. However, the calculated **5a**/**5b** and **5c**/**5d** population ratios were only moderately different from experimental values. These conclusions were supported by the NMR observation of only two conformers of type **5a** and **5b** for peracetylobtusallene III (**6**) in $CDCl_3$. One wonders whether a similar dependence of equilibria on the solvent nature applies to the cytotoxic macrolide bryostatin 10, where intramolecular H-bonding occurs both in the crystal and in $CDCl_3$ solution.[13] In any event, any dependence of the conformational state on the nature of the medium, as in the present case, is worthy of attention as a general indication to help in unravelling the factors involved in recognition interactions. The "hydrophobic collapse" of the antitumour agent taxol serves as a lesson.[4]

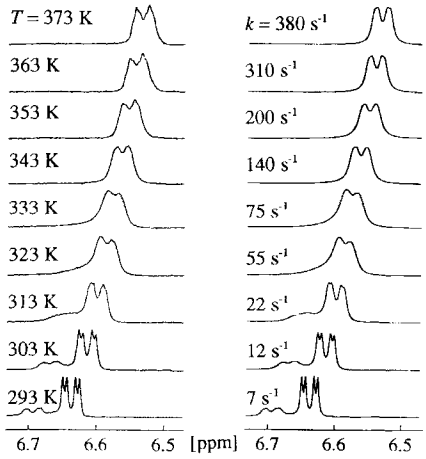

Figure 1. Experimental (in $(CD_3)_2SO$; left) and DNMR 5-calculated (right) ^1H NMR lineshape for the H 1 signal of conformers **3a** and **3b** in equilibrium.

Activation barriers: Activation barriers for conformational processes involving **1**, **4** and **5** (*Schemes* 1, 3, 4) were evaluated from dynamic NMR experiments in $CDCl_3$ in a temperature range from $-50\,^\circ C$ to $+50\,^\circ C$. Because of relatively high coalescence temperatures for both **2** and **3**, a high-boiling-point solvent like $(CD_3)_2SO$ had to be used, enabling us to raise the temperature to $+130\,^\circ C$ and thus to examine these systems in the whole range from slow to fast exchange. A digression is in order here: on heating compound **2** in $(CD_3)_2SO$ in the NMR probe at temperatures above $110\,^\circ C$, **3** was formed in low yield, besides much polymeric material, while the mixture turned a reddish colour. When **2** was heated, under otherwise identical conditions, in the presence of added 3,4-dihydro-2-pyran, the latter was converted into mainly tetrahydro-2-furaldehyde while no **3** could be detected at HPLC-UV sensitivity level. Moreover, dihydropyran proved stable when heated alone in $(CD_3)_2SO$. Though not ruling out a free-radical process, these observations may be rationalized by a sequential electrophilic attack of BrOH at the enol ether double bond, opening of the resulting bromohydrin to give 2-bromo-5-hydroxypentanal, and intramolecular nucleophilic replacement of the bromine atom by the hydroxyl group.

Lineshape analysis through the DNMR 5 program[14] of the H 1 signal for either **2** or **3** (only the latter case is exemplified in Figure 1) gave $\Delta G^{\ddagger}_{298K} = 16.3 \pm 0.2$ and 16.1 ± 0.2 kcal mol^{-1}, respectively. Kinetic parameters were calculated from the Eyring plot with transmission coefficient $k = 1$ and $T = 298$ K; this gave $\Delta H^{\ddagger} = 10.7$ kcal mol^{-1} and $\Delta S^{\ddagger} = -18.1$ e.u. Overlapping of signals hindered the same type of analysis for **4**, where the rough equation $k_c(T_c) = \pi \Delta\nu/\sqrt{2}$[15] was used to obtain, from the absolute rate theory with transmission coefficient $k = 1$, $\Delta G^{\ddagger}_{298K} = 13.3 \pm 0.4$ kcal mol^{-1}. Kinetic parameters for 180° olefinic-bond flipping are similar for **1**, **4** and **5** in the same solvent, as deduced from the coalescence temperature for some ^1H NMR signals of **5** (on the assumption that $\Delta\delta_H$ is similar to that for **4**). This allowed us to estimate $\Delta G^{\ddagger}_{298K} = 13.0 \pm 0.5$ kcal mol^{-1}.

Here the results of MM calculations proved to be critically dependent on the choice of the dihedral angle, in any case leading to overestimation of the activation barriers by 4–5 kcal mol^{-1}. The only exception concerned the **5c**$\rightleftharpoons$**5d** equilibrium where, by rotation of the dihedral angle O-C4-C5-C6 from -130° to $+80^\circ$, a correct estimate of the activation barrier was obtained. For equilibria of type **a** $\rightleftharpoons$ **c** and **b** $\rightleftharpoons$ **d** (Schemes 3 and 4) we obtained $\Delta H^{\ddagger}_{calcd} < 10$ kcal mol^{-1}.

Conclusions

The behaviour of unsaturated *O*-bridged 12-membered-ring C_{15} acetogenins in solution is replete with intricacies that had been previously overlooked,[7] probably because conformer signals were mistaken for impurity signals. The rules governing these systems can be summarized as follows.

1) *Trans* olefinic bonds undergo 180° flipping, by which conformers are intercoverted. These equilibria are controlled by enthalpic factors and are only slightly dependent on the solvent nature. Activation barriers depend on the ring size, being larger for compounds with a 10-membered (**2**–**3**) than an 11-membered (**1**–**4**–**5**) subunit ring.
2) The above systems are also subjected to faster conformational motions, which result in averaged vicinal J couplings. When 1,3-dihydroxy substituents are present, control of these equilibria depends on the solvent nature; in nonpolar solvents this occurs through intramolecular H-bonding between the hydroxy groups, by which two extra, intramolecularly H-bonded conformers come into play. In polar hydrogen-bonding solvents, control occurs through solute–solvent H-bonding, by which the conformers arising from 180° flipping of the olefinic bond, and having the 1,3-dihydroxy groups in the thermodynamically favoured pseudoequatorial position, take greater weight.
3) The present study, together with previous studies for 9-membered xenicane diterpenes[16] and 12-membered carbocycles,[17] shows that stepwise shrinking of the ring from 12- to 9-membered is smoothly attended by an increase of the activation barrier by 3–4 kcal mol^{-1} for each step. In this ring size range the value of the barrier is determined just by the ring size, while the nature of the substituents is immaterial.

Experimental Procedure

General methods: Melting points were recorded with a Kofler hot stage microscope and are uncorrected. Flash chromatography (FC) was performed on Merck Si-60, 15–25 μm, TLC on Merck Kieselgel 60 PF_{254} plates, HPLC on Merck LiChrosorb Si60 (7 μm), reversed-phase HPLC on Merck LiChro-

spher RP8 (7 μm), in both last cases 25 × 1 cm columns, solvent flux 5 mL min^{-1}, and UV monitoring at $\lambda = 220$ nm. UV spectra were taken with a Perkin–Elmer Lambda-3 spectrophotometer and CD spectra with a Jasco J710 spectropolarimeter. Polarimetric data were measured with a JASCO-DIP-181 polarimeter; $[\alpha]_D$ values were reported in 10^{-1} °mL g^{-1}. Unless otherwise stated, NMR spectra were recorded at 299.94 MHz (^{1}H) or 75.43 MHz (^{13}C, Varian XL-300 spectrometer) relative to internal Me_4Si ($\delta = 0$) and J in Hz (derived from differential spin decoupling[18]) in $CDCl_3$ at probe temperature +20 °C, unless otherwise stated. For variable-temperature experiments either $(CD_3)_2SO$ or $CDCl_3$ were used as solvents. COSY 60 experiments[19] for **4** were carried out at −60 °C. Saturation-transfer experiments were carried out with the same standard pulse sequence used for NOE experiments. The ^{1}H NMR probe for high-temperature measurements was calibrated at ±1 °C. NMR line shape simulation was performed with the DNMR 5 computer program.[14] Molecular mechanics (MM) calculations were carried out first with GLOBAL-MMX (GMMX) computer program to search for conformational space and then refined with PCMODEL 4.0 computer program (Serena Software, Bloomington, Indiana), both based on the MMX force field. Starting conformations were drawn from Dreiding models and minimizations were carried out by assuming a dielectric constant $\varepsilon = 1.5$; for **5** calculations were also carried out for the dielectric values of either $CHCl_3$ or CH_3OH. The C=C–C–H and C=C–C–C torsional parameters were changed from (V1 = 0.0, V2 = 0.0, V3 = −0.24) and (V1 = −0.44, V2 = 0.24, V3 = 0.06) to (V1 = 0.0, V2 = 0.0, V3 = −0.30) and (V1 = −0.54, V2 = 0.44, V3 = −0.60), respectively.[10]

Isolation of compounds: Obtusallenes I–IV were isolated from air-dried samples of the red seaweed *Laurencia obtusa* collected either near Kaş, Antala, in the Turkish Mediterranean in October 1987[7d] (400 g) or recollected there (Collection no. 752M, 250 g) in summer 1994. Work-up of the latter sample was similar to the first one:[7c] the CH_2Cl_2/MeOH (2:1) extract, 7 g, was subjected to FC with *n*-hexane/EtOAc gradient elution, which yielded 21 fractions. Previously overlooked obtusallene IV (**1**) was obtained from fraction 3 and further purified by Si 60 HPLC with *n*-hexane/EtOAc 95:5. Obtusallene I (**2**)[7a, 7b, 7c] and 10-bromoobtusallene I (**3**)[7d] were recrystallized from *n*-hexane before spectral measurements. Obtusallene II (**4**)[7c] was purified by TLC with *n*-hexane/AcOEt 85:15. Obtusallene III (**5**)[7c], which proved rather unstable in $CDCl_3$ solution, was purified by TLC with AcOEt/MeOH 10:1. As well as from the Turkish *L. obtusa*,[7c] obtusallene II (**4**) was also isolated from *L. microcladia* collected at Il Rogiolo;[9, 12] fractions 11–18 from the *n*-hexane extract[9] were subjected to reversed-phase HPLC with MeCN/H_2O (65:35) followed by HPLC with *n*-hexane/Et_2O (75:25), obtaining **4** (t_R = 5.0 min, 6.0 mg, 0.016%) with NMR spectra and chiroptical data matching those previously reported.[7c]

Obtusallene IV (1): UV (MeOH): λ_{max} (ε) = 204 nm (21800 mol^{-1} L cm^{-1}); CD (MeOH): $\Delta\varepsilon_{max}$ (211 nm) = +35.1; $[\alpha]_D^{20}$ = +247 (c = 0.23, MeOH); ^{1}H NMR ($CDCl_3$, −40 °C): δ = 6.00 (dd, $J_{1,3}$ = 5.6, $J_{1,4}$ = 1.7, H1), 5.34 (dd, $J_{3,1}$ = 5.6, $J_{3,4}$ = 6.6, H3), 4.18 (dddd, $J_{4,1}$ = 1.7, $J_{4,5}$ = 9.8, $J_{4,3}$ = 6.6, $J_{4,5\beta}$ = 2.0, H4), 1.59 (ddd, $J_{5\alpha,6}$ = 2.0, $J_{5\alpha,4}$ = 10.1, J_{gem} = 14.2, H_α5), 1.68 (ddd, $J_{5\beta,6}$ = 10.5, $J_{5\beta,4}$ = 2.0, J_{gem} = 14.2, H_β5), 3.95 (dt, $J_{6,5\beta}$ = 10.5, $J_{6,7}$ = $J_{6,5\alpha}$ = 2.0, H6), 4.38 (dt, $J_{7,8\alpha}$ = 2.5, $J_{7,8\beta}$ = $J_{7,6}$ = 2.0, H7), 2.40 (m, $H_2$8), 4.70 (dt, $J_{9,10}$ = 5.5, $J_{9,8\alpha}$ = 8.8, $J_{9,8\beta}$ = 7.4, H9), 4.46 (ddd, $J_{10,9}$ = 5.5, $J_{10,11\alpha}$ = 12.0, $J_{10,11\beta}$ = 3.7, H10), 2.44 (ddd, $J_{11\alpha,10}$ = 12.0, $J_{11\alpha,12}$ = 10.0, J_{gem} = 14.8, H_α11), 2.86 (ddd, $J_{11\beta,10}$ = 3.6, $J_{11\beta,12}$ = 1.7, J_{gem} = 14.8, H_β11), 5.78 (ddd, $J_{12,11\alpha}$ = 10.0, $J_{12,11\beta}$ = 1.7, $J_{12,13}$ = 15.8, H12), 5.67 (dd, $J_{13,14}$ = 5.1, $J_{13,12}$ = 15.8, H13), 4.38 (qd, $J_{14,15}$ = 6.6, $J_{14,13}$ = 5.1, H14), 1.30 (d, $J_{15,14}$ = 6.6); NOE: H4 with H3, H_β5 and $H_3$15; H_β5 with H6 and H7; H6 with H7 and H_α8; H9 with H_β8; H13 with H6, H_α11 and $H_3$15; $H_3$15 with H3, H4, H12 and H13; ^{13}C NMR ($CDCl_3$, −10 °C): δ = 73.70 (d, C1), 200.74 (s, C2), 103.32 (d, C3), 64.45 (d, C4), 36.74 (t, C5), 76.52 (d, C6), 62.48 (d, C7), 37.59 (t, C8), 77.99 (d, C9), 49.88 (d, C10), 38.53 (t, C11), 128.22 (d, C12 or C13), 128.08 (d, C13 or C12), 70.53 (d, C14), 14.01 (q, C15); MS (70 eV, EI): m/z (%) = 345/347/349 (12/15/5) $[M - Br]^+$, 307/309/311 (21/27/7) $[M - C_3H_2Br]^+$, 227/229 (100/51) $[M - C_3H_2Br - HBr]^+$, 191 (29), 147 (35), 119 (19), 81 (28); HR-MS-EI: calcd for $C_{12}H_{17}BrClO_2$ $[M - C_3H_2Br]^+$: 307.0056; found 307.0053 ± 0.001; MS (CI, NH_3): m/z (%) = 440/442/444/446 (10/45/57/30) $[M + NH_3]^+$, 425/427/429/431 (12/51/65/36), $[M + H]^+$, 407/409/411/413 (21/70/77/56) $[M + H - H_2O]^+$, 389/391/393 (18/36/18) $[M + H - HCl]^+$, 371/373/375 (15/30/15) $[M + H - HCl - H_2O]^+$.

Obtusallene I (2): Previously unavailable[7a, 7d] or amended data only are reported here. UV (MeOH): λ_{max} (ε) = 205 nm (20600 mol^{-1} L cm^{-1}); CD (MeOH): $\Delta\varepsilon_{max}$ (214 nm) = −31.6.

10-Bromoobtusallene I (3): M.p. 145–146 °C; UV (MeOH): λ_{max} (ε) 205 nm (27000 mol^{-1} L cm^{-1}); CD (MeOH): $\Delta\varepsilon_{max}$ (218 nm) = −46.5.

Obtusallene II (4): UV (MeOH): λ_{max} (ε) = 204 nm (20400 mol^{-1} L cm^{-1}); CD (MeOH): $\Delta\varepsilon_{max}$ (218 nm) = −16.8. At the fast exchange limit (+51 °C), the ^{1}H NMR spectrum of **4** was superimposable on that previously reported;[7d] in Table 5, last row, coupling assignments and small differences in J values with respect to the literature are reported.[7d] ^{13}C NMR ($CDCl_3$, +51 °C, fast exchange limit): δ = 73.42 (d, C1), 200.63 (s, C2), 102.99 (d, C3), 76.65 (d, C4), 37.78 (t, C5), 80.35 (d, C6), 61.32 (brd, C7), 40.36 (brt, C8), 51.57 (d, C10), 39.26 (brt, C11), 129.56 (brd, C12), 132.42 (brd, C13), 21.22 (q, C15). Resonances were not detected for either C9 or C14 because of extremely broad line shape.

Minor conformer 4a: ^{1}H NMR ($CDCl_3$, −60 °C, slow exchange limit): δ = 6.00 (d, J = 5.5, H1), 5.34 (t, J = 5.5, H3), 4.05 (m, H4), 2.20 and 1.78 (m, $H_2$5), 4.00 (m, H6), 4.43 (td, J = 1.7, 4.8, H7), 2.20 and 2.12 (m, $H_2$8), 4.77 (td, J = 6.3, 8.5, H9), 4.49 (m, H10), 2.86 (td, J = 2.5, 14.6, H11β), 2.40 (td, J = 9.5, 14.6, H11α), 5.98 (m, H12), 5.90 (m, H13), 3.90 (m, H14), 1.33 (d, J = 6.6, $H_3$15); ^{13}C NMR ($CDCl_3$, −51 °C, slow exchange limit): δ = 73.49 (C1), 200.63 (C2), 102.43 (C3), 78.53 (C4), 37.92 (C5), 80.98 (C6), 64.02 (C7), 36.67 (C8), 51.11 (C10), 37.92 (C11), 126.52 (C12), 133.28 (C13), 21.57 (C15).

Major conformer 4d: ^{1}H NMR ($CDCl_3$, −60 °C, slow exchange limit): δ = 6.04 (d, J = 5.5, H1), 5.51 (t, J = 5.5, H3), 4.39 (m, H4), 2.05 (dd, J = 11.5, 14.9, H5β), 1.88 (ddd, J = 2.0, 6.6, 14.9, H5α), 4.25 (dd, J = 6.2, 10.5, H6), 4.62 (t, J = 6.2, H7), 2.32 and 1.78 (m, $H_2$8), 3.94 (m, H9), 4.51 (m, H10), 2.77 (m, $H_2$11), 5.90 (m, H12), 5.46 (m, H13), 3.98 (m, H14), 1.26 (d, 6.6, $H_3$15); ^{13}C NMR ($CDCl_3$, −51 °C, slow exchange limit): δ = 74.06 (C1), 200.63 (C2), 102.95 (C3), 78.88 (C4), 37.09 (C5), 80.45 (C6), 59.53 (C7), 37.92 (C8), 50.67 (C10), 41.74 (C11), 129.01 (C12), 135.03 (C13), 21.86 (C15).

Obtusallene III (5): UV (MeOH): λ_{max} (ε) = 204 nm (19600 mol^{-1} L cm^{-1}); CD (MeOH): $\Delta\varepsilon_{max}$ (221 nm) = −16.6. At the fast exchange limit (+51 °C) the ^{1}H NMR spectrum for **5** in $CDCl_3$ was superimposable on that previously reported.[7d] except for small differences in J patterns as indicated in the penultimate row of Table 5. ^{1}H NMR (CD_3OD, +51 °C, fast exchange limit): δ = 6.23 (dd, J = 5.5, 2.0, H1), 5.55 (t, J = 5.5, H3), 4.39 (m, H4 and H12), 5.89 (dd, J = 7.2, 15.0, H5), 5.97 (dd, J = 5.0, 15.0, H6), 4.13 (ddd, J = 2.0, 5.0, 10.4, H7), 2.29 (td, J = 10.4, 13.4, H8β), 2.00 (tdd, J = 2.1, 4.7, 13.4, H8α), 3.74 (m, H9, H10 and H13), 2.10 (ddd, J = 5.5, 10.5, 13.0, H11β), 1.68 (brdd, J = 4.0, 13.0, H11α), 3.70 (dq, J = 8.0, 6.6, H14), 1.26 (d, J = 6.6, $H_3$15); ^{13}C NMR ($CDCl_3$, 51 °C, fast exchange limit): δ = 73.41 (d, C1), 202.03 (s, C2), 102.29 (d, C3), 71.53 (d, C4), 126.64 (brd, C5), 135.10 (brd, C6), 79.83 (brd, C7), 40.11 (brt, C8), 69.16 (brd, C9), 71.42 (brd, C10), 38.47 (brt, C11), 72.39 (d, C12), 86.24 (brd, 13-C), 76.28 (brd, C14), 18.81 (q, C15).

Acknowledgments: We are grateful to A. Sterni for his skilled technical contribution with mass spectra and to MURST (Progetti 40%) and CNR (Roma) for financial support.

Received: February 25, 1997 [F624]

[1] M. Satake, S. Ishida, T. Yasumoto, M. Murata, H. Utsumi, T. Hinomoto, *J. Am. Chem. Soc.* **1995**, *117*, 7019–7020.
[2] H. U. Tingmo, J. M. Curtis, J. A. Walter, J. L. C. Wright, *J. Chem. Soc. Chem. Commun.* **1995**, 597–599.
[3] K. L. Erickson in *Marine Natural Products, Vol. 4* (Ed.: P. J. Scheuer), Academic Press, New York, **1983**, p. 131.
[4] Q. Gao, W. L. Parker, *Tetrahedron* **1996**, *52*, 2291–2300.
[5] K. C. Nicolaou, F. P. Y. T. Rutjes, E. A. Theodorakis, J. Tiebes, M. Sato, E. Untersteller, *J. Am. Chem. Soc.* **1995**, *117*, 1173–1174; M. Bratz, W. H. Bullock, L. Overman, T. Takemoto, *J. Am. Chem. Soc.* **1995**, *117*, 5958–5966.
[6] G. Guella, F. Pietra, *Helv. Chim. Acta* **1991**, *74*, 47–54.
[7] a) P. J. Cox, S. Imre, S. Islimyeli, R. H. Thomson, *Tetrahedron Lett.* **1982**, *23*, 579–580; b) P. J. Cox, R. A. Howie, *Acta Crystallogr.* **1982**, *B38*, 1386–1387;

c) A. Öztunç, S. Imre, H. Lotter, H. Wagner, *Phytochemistry* **1991**, *30*, 255–257; d) A. Öztunç, S. Imre, H. Wagner, M. Norte, J. J. Fernández, R. González, *Tetrahedron* **1991**, *47*, 2273–2276; e) A. Öztunç, S. Imre, H. Wagner, M. Norte, J. J. Fernandez, R. Gonzalez, poster at the 39th Annual Congress on Medicinal Plant Research, Saarbrücken, **1991**.

[8] J. Dale, *Top. Stereochem.* **1976**, *9*, 199–270.

[9] G. Guella, G. Chiasera, I. Mancini, F. Pietra, *Helv. Chim. Acta* **1990**, *73*, 1612–1620.

[10] J. L. Broeker, R. W. Hoffmann, K. N. Houk, *J. Am. Chem. Soc.* **1991**, *113*, 5006–5017.

[11] C. A. G. Haasnoot, F. A. A. M. De Leeuw, C. Altona, *Tetrahedron* **1980**, *36*, 2783–2792.

[12] G. Guella, I. Mancini, G. Chiasera, F. Pietra, *Helv. Chim. Acta* **1991**, *74*, 774–786.

[13] Y. Kamano, H.-p. Zhang, H. Morita, H. Itokawa, O. Shirota, G. R. Pettit, D. L. Herald, C. L. Herald, *Tetrahedron* **1996**, *52*, 2369–2376.

[14] C. B. LeMaster, C. L. LeMaster, H. S. True, *Quantum Chem. Prog. Exch.* **1989**, QCMP 059, Indiana University.

[15] G. Binsch in *Dynamic Nuclear Magnetic Resonance Spectroscopy* (Eds.: L. M. Jackman, F. A. Cotton), Academic Press, New York, **1975**, pp. 45–81; D. Kost, E. H. Carlson, M. Raban, *J. Chem. Soc. Chem. Commun.* **1971**, 656–657.

[16] G. Guella, G. Chiasera, I. N'Diaye, F. Pietra, *Helv. Chim. Acta* **1994**, *77*, 1203–1221.

[17] F. A. L. Anet, T. N. Rawdah, *J. Am. Chem. Soc.* **1978**, *100*, 5003–5007.

[18] J. K. M. Saunders, J. D. Mersh, *Prog. NMR Spectrosc.* **1982**, *15*, 353–400.

[19] A. Bax, R. Freeman, *J. Magn. Reson.* **1981**, *44*, 542–561.